Volume Changes and Relaxations Within the Interphase Domain of Blendlike Polymer Particles

ÖNDER PEKCAN

Department of Physics, Istanbul Technical University, Maslak, 80626, Istanbul, Turkey

SYNOPSIS

The behavior of volume changes upon solvent swelling and annealing was studied within the interphase domain of poly(methyl methacrylate) (PMMA) particles sterically stabilized with polyisobutylene (PIB). Transient fluorescence technique was applied on these micron-sized particles labeled in the PMMA phase with naphthalene (N) groups. Mean decay times $\langle \tau \rangle$, obtained from fluorescence decay measurements, were used to examine volume changes within the PMMA–PIB interphase domain. The mathematical model proposed by Inokuti–Hirayama for the quenching of lifetimes was employed to quantify the individual volume changes and relaxations at this particular domain. © 1995 John Wiley & Sons, Inc.

INTRODUCTION

Some commercially used polymeric systems are composed of two separate phases, which come through blending or phase separation in graft or block copolymers. It would be interesting to make experiments sensitive to phenomena occurring only within individual phases of the material. The fluorescence labeling method allows one to make such experiments. For about a decade the transient fluorescence technique has been used to examine the internal morphology of such blendlike materials.[1-5]

In this manuscript we describe how one can use fluorescence spectroscopy, particularly fluorescence decay measurements, to examine detailed relaxation behavior of the glassy phase of blendlike poly(methyl methacrylate) (PMMA) particles. These particles are spherical and usually prepared by dispersion polymerization of methyl methacrylate (MMA) in cyclohexane in the presence of butyl rubber.[6] The major component in this type of particle, PMMA homopolymer of broad molecular weight distribution, is present at about 95–97% by weight. During the reaction, grafting occurs between the butyl rubber and the growing PMMA chains. Most of the graft copolymer is buried in the particle interior, where it forms an interconnected network[2,4] of polyisobutylene (PIB). Some graft copolymer forms a monolayer on the particle surface, which serves as the steric stabilizer. Thus, these particles have an interpenetrating networklike global morphology. This global feature of the morphology has been of interest and studied carefully.[2-4] Thus, while PIB and PMMA are incompatible polymers and phase separate, they are still held together over macromolecules dimensions by covalently bonding between them. The nature of the interface between PIB and PMMA phases, where they mix and form an interphase domain, was studied using transport experiments involving fluorescence quenching and energy transfer.[7] A pictoral representation of PMMA particle and interphase domain are shown in Figure 1.

In this manuscript we pose questions about how one can use fluorescence labeling techniques to obtain detailed information about the individual phases in PMMA particle. Here, we focus on volume changes and volume relaxation within the interphase domains, as a function of annealing temperature and sample history, determined by fluorescence decay measurements.

Operationally, the PMMA phase in the particle is labeled by incorporating a comonomer containing a naphthalene group (N) in the methyl methacrylate polymerization step of particle preparation. The co-

Journal of Applied Polymer Science, Vol. 56, 1527–1536 (1995)
 CCC 0021-8995/95/121527-10

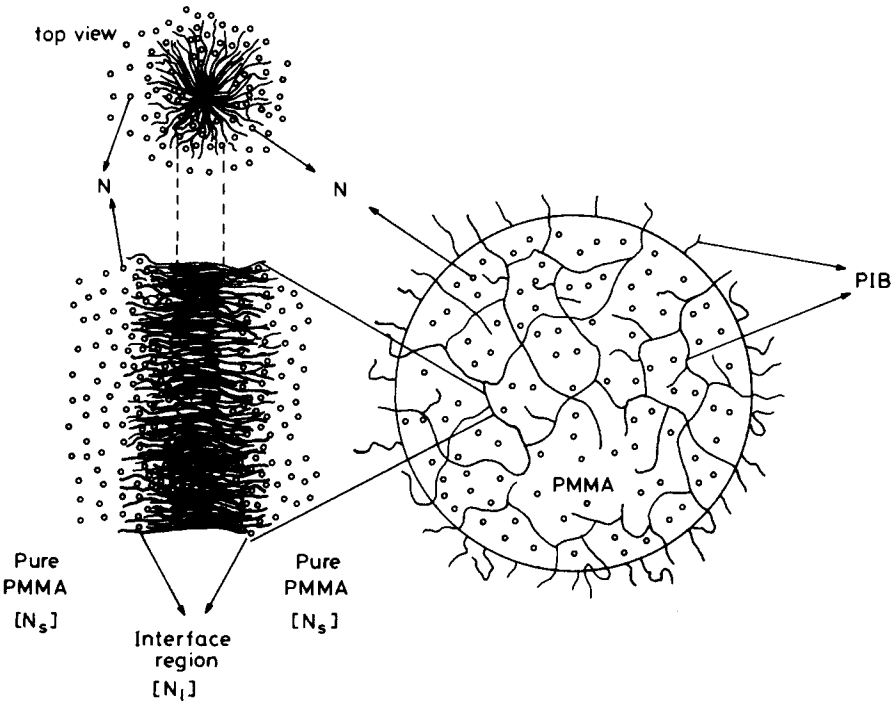

Figure 1 Pictural representation of *N*-labeled, PMMA particle with the magnified part of the interphase domain.

monomer, 1-naphthylmethyl methacrylate, has a reactivity ratio somewhat less than unity for copolymerization with MMA. Hence, if MMA is in excess, the tendency will be against blocks of N units. The assumption of a statistical distribution of N groups within the PMMA chains is reasonable.

We examine two labeled materials. One with a monomer mol ratio of approximately 13 : 100 : 2 for IB : MMA : N is referred to as N2; the other, of approximately 13 : 100 : 10, as N10. When their fluorescence spectra and decay profiles are compared to those of 1-naphthyl-methyl pivalate (NMP), which serves as a model for the N groups in the particles, we find out that the fluorescence decay time of the N groups is very sensitive to N-content of the PMMA phase. Self-quenching, Eq. (1), leads to dissipation of some of the electronic excitation energy as heat.

$$N^* + N \rightarrow 2N \qquad (1)$$

Factors that decrease the mean separation of N groups increase the extent of self-quenching. The decay time of N fluorescence becomes shorter. Conversely, swelling of the interphase domains increases the mean N-group separation. The fluorescence decay time gets longer. These observations can be interpreted quantitatively. Consequently, these measurements provide a powerful new tool for studying volume deformation within a single phase of a multicomponent material.

EXPERIMENTAL

The preparation, purification, and characterization of N2 and N10 have been previously reported.[8] Samples were freeze dried from cyclohexane and stored as a powder. Dispersions in alkane solvents (ca 3–5 mg/mL) were prepared by sonicating the mixture for 1 or 2 min in an ultrasonic cleaning bath. These samples, in 12 mm o.d. quartz tubes fitted with a graded seal, were degassed by several freeze–pump–thaw cycles and sealed under vacuum. Powder samples were placed in 3 mm i.d. quartz tubes and sealed under vacuum.

Fluorescence decay profiles were measured by the time-correlated single photon counting technique, exciting the samples at 280 mm, and observing the emission through an interference filter at 337 nm. The samples were turbid to opaque. Although the excitation and emission optics were at 90° to one another, the samples often had to be positioned so that one measured essentially front face fluores-

cence. Fluorescence decays for these samples were nonexponential, but in our purpose could be fit to a sum of two exponential terms. The goodness of the fitting of the data to the model was determined by χ^2 (which is less than 1.5 in all fits).

During the experiments, the samples were heated to the annealing temperature and kept there for 2 to 3 h in an oven. Each sample was allowed to cool to room temperature, and the fluorescence decay profiles $I(t)$ were remeasured. The samples were then reheated to the next higher annealing temperature, allowed to cool, and remeasured. All measurements reported here were carried out at room temperature (25°C).

RESULTS AND DISCUSSION

The fluorescence spectra of N2 and N10 are shown in Figure 2. Even though the mean local concentration of N groups in N10 is quite high (ca. 0.9 M), relatively little excimer emission is seen. As we point out below, substantial self-quenching occurs. We conclude that most of the self-quenching interactions involve N–N separations or mutual orientations, which do not lead to excimer fluorescence.

A fluorescence decay traces of N2 and N10 are shown in Figure 3. Although nonexponential in form, they can be well fit to a sum of two exponential terms

$$I(t) = A_s e^{-t/\tau_s} + A_l e^{-t/\tau_l} \quad (2)$$

We refer to the long component lifetime as τ_l, with a prefactor A_l, and the short component lifetime as τ_s with a prefactor A_s. In some samples, a very short additional component was detected in $I(t)$ and was attributed to light scattering.

When samples of N2 and N10 were heated, the lifetimes measured at elevated temperatures were found to be shorter than those at room temperature.[9] Upon cooling to room temperature, we noticed that the lifetimes were substantially different from their initial values.[10] This behavior depended upon the annealing temperature as well as the form of the sample. The effects of annealing temperature on three samples are shown in Figure 4. Prior heating to temperatures below 60°C has little effect on the room temperature lifetimes. Above 60°C, irreversible changes occur in both τ_l and τ_s. For samples of N2 and N10 in powder form, these lifetimes decrease monotonically with increasing annealing temperature. For dispersions in hexadecane or isooctane, τ values first increase for annealing temperatures up to ca. 110°C and subsequently decrease.

Figure 5 demonstrates corresponding effects of sample heating on the prefactor ratio A_l/A_s. For the powder sample, this ratio remains constant up to 80°C, then decreases monotonically. The hexadecane dispersion shown an increase of A_l/A_s for annealing between 70°C to 100°C, with heating to

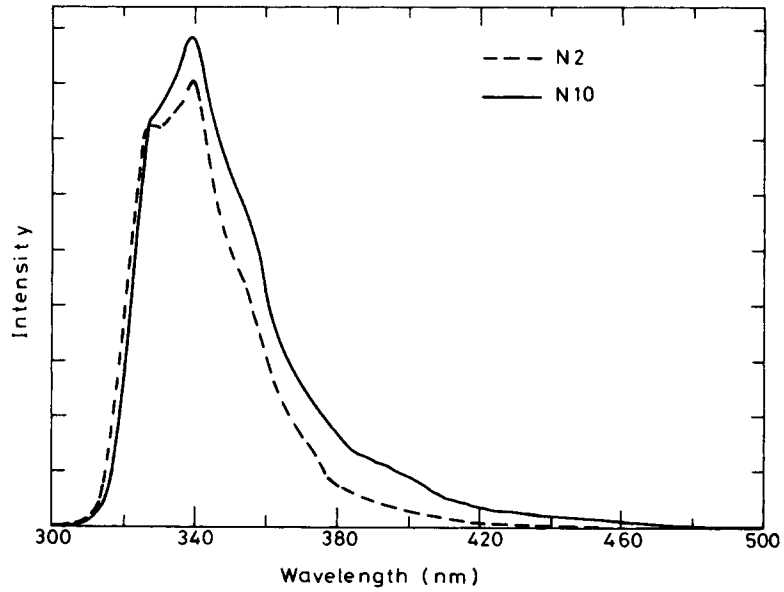

Figure 2 Fluorescence spectra of N2 and N10 as dispersions in isooctane at 25°C λ_{ex} = 280 nm.

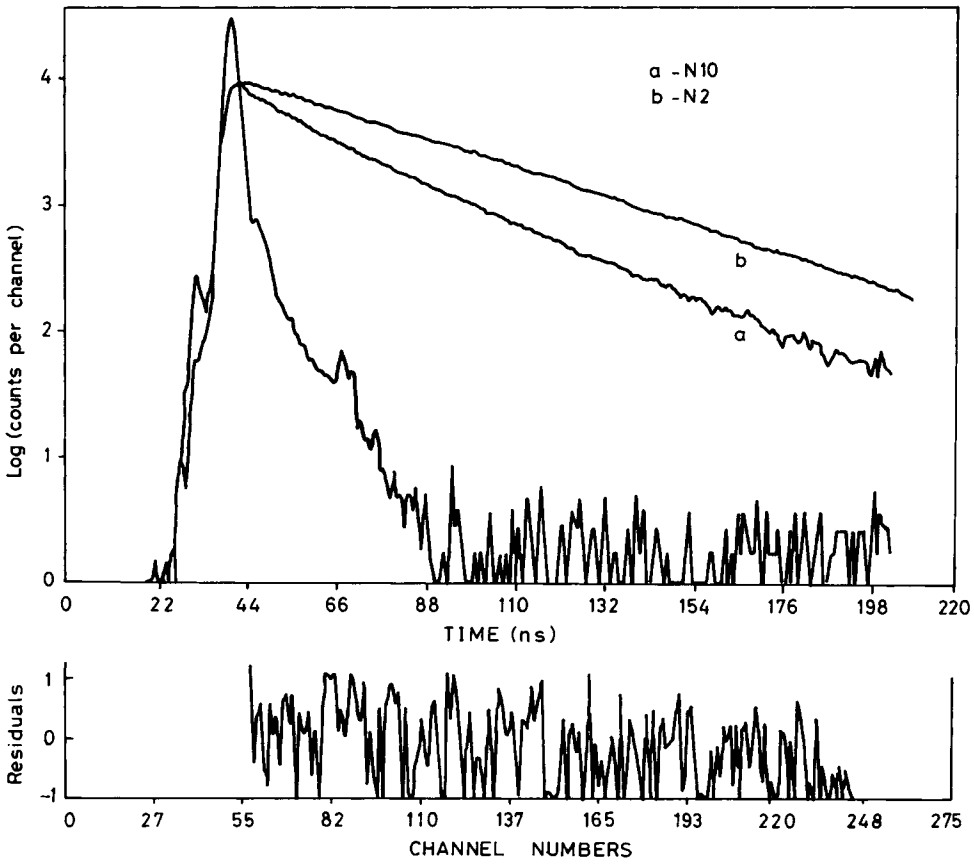

Figure 3 Fluorescence decay profile of N2 and N10 sample in isooctane at 25°C, λ_{ex} = 280 nm; λ_{em} = 337 nm.

higher temperatures, leading to a decrease in the ratio.

In Figures 4 and 5 we observe that various kinds of sample treatments effect the fluorescence decay profiles of naphthalene labels in the PMMA phase. These decay rates are faster than those of suitable model compounds such as NMP in PMMA, and the decay rates increase with increasing concentration of N. These are the characteristics of fluorescence self-quenching (or concentration quenching), terms that refer to any phenomenon of the form [$N^* + N \rightarrow 2N$]. Mechanistically, such an interaction might involve formation of an excimer (nonemissive), followed by intersystem crossing to the triplet state. Irrespective of these details, the major conclusion we wish to draw is that the fluorescence profiles we measure are sensitive to the distribution of N groups in the PMMA phase of the interphase domain. Factors that cause swelling of this domain will lead to an increase in the separation of N groups and a slower rate of fluorescence decay. Factors that induce contraction to interphase domain, decrease the separation of N groups, giving a faster rate of fluorescence decay. Thus, the changes in τ_l and τ_s observed in Figure 3 reflect volume changes in the PMMA phase.

Although this qualitative description is on firm ground, a more quantitative interpretation requires recourse both to a model and a number of simplifying assumptions. These can be treated at different levels of sophistication. Our approach here is to briefly review the static quenching model for fluorescence and phosphorescence quenching and to present one simplified application of this model to our data. This exercise is useful in demonstrating the power of insight of the fluorescence decay technique.

Static Quenching Models

An active-sphere model for excited state quenching in the absence of diffusion was proposed by Perrin.[11] It describes the general reaction [$N^* + Q \rightarrow N + Q$ or Q^*], of which self-quenching is a special case. In this model, N^* is quenched instantaneously by a

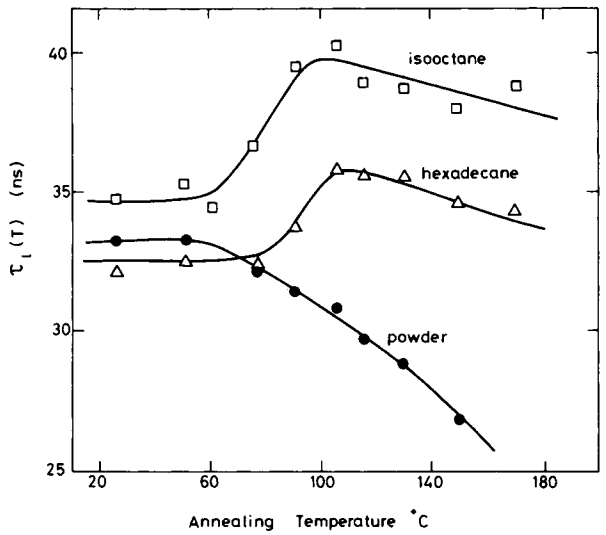

Figure 4 Plot of τ_1 for N10 measured at 25°C for samples annealed 3 h successively at each of the temperatures indicated: (●) dry powder sample; (△) dispersion 6 mg/mL in hexadecane; (□) dispersion 6 mg/mL in isooctane.

quencher Q inside the sphere, but unaffected by one outside. This model accommodates the observation that fluorescence and phosphorescence intensities decrease as quencher concentration increases. The Perrin model also predicts that the unquenched species have the same lifetime τ_0 as N groups at zero quencher concentration. This prediction is at odds with triplet lifetime studies in son

Dexter's Theory of energy transfer by the exchange mechanism.[14] Here, the rate constant for quenching (or self-quenching), $k_q(r)$ depends upon the distance r between N^* and the quencher. A convenient way of summarizing these results in terms of the equation

$$k_q(r) = (1/\tau_0)\exp\{\gamma[1 - (r - R_0)]\} \qquad (3)$$

where τ_0 is the fluorescence lifetime in the absence of quencher, and

$$\gamma = 2R_0/L \qquad (4)$$

L is the "effective average Bohr radius" and takes a value of 1.4 Å, R_0 is the critical transfer distance. Note that when $r = R_0$, $k_q(r) = 1/\tau_0$, and the quenching rate equals the decay rate of the isolated excited state. Because $k_q(r)$ is distance dependent, fluorescence decays in the absence of mass diffusion will, in general, not be exponential. The form of the decay will depend upon the spatial distribution of quenchers. Assuming a random spatial distribution, the fraction of excited states surviving at time t is described by

$$I(t) = \exp\left(-\frac{t}{\tau_0} - \frac{[N]}{[N_0]}\frac{g(e^{\gamma}t/\tau_0)}{\gamma^3}\right) \qquad (5)$$

where, for z significantly larger than 1,

$$g(z) = (\ln z)^3 + 1.73(\ln z)^2 + 5.93(\ln z) + 5.44 + \cdots \qquad (6)$$

Here, $[N]$ is the quencher concentration and $[N_0]$ is the critical transfer concentration defined by

$$[N_0] = 3/(4\pi R_0^3) \qquad (7)$$

which, in units of moles per liter takes the value

$$R_0 = 7.346[N_0]^{-1/3}(\text{Angstroms}) \qquad (8)$$

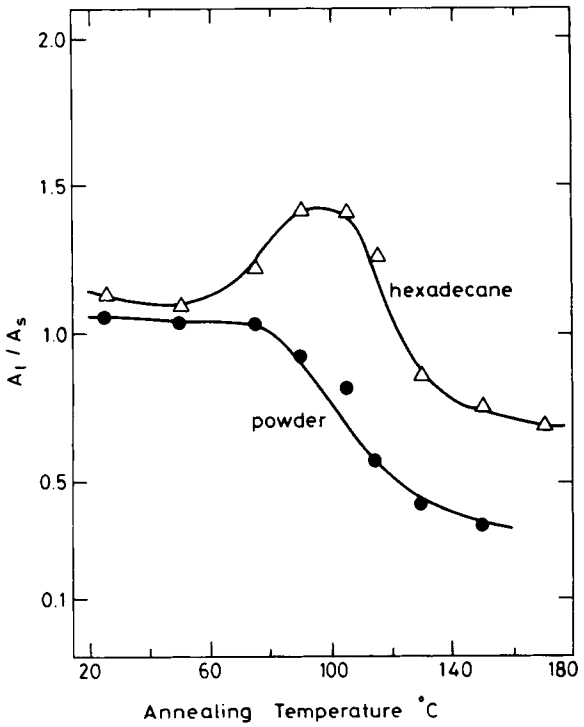

Figure 5 Plot of A_1/A_s for N10 determined from fluorescence decay measurements at 337 nm and 25° for samples annealed 3 h at each temperature indicated.

Equation (5) predicts nonexponential decays. Semilogarithmic plots of numerically generated decay profiles by IH[13] show curvature, which become pronounced only at short times ($t/\tau_0 < 0.5$). As IH point out, it is sometimes more useful to talk about the mean decay time, $\langle\tau\rangle$, defined by

$$\langle\tau\rangle = \int_0^\infty I(t)\,dt \Big/ \int_0^\infty I(t)\,dt \qquad (9)$$

These mean decay times decrease with increasing quencher concentration. In Figure 6 we plot ($\langle\tau\rangle/\tau_0$) vs. ($[N]/[N_0]$), calculated numerically by IH using Eqs. (5) and (9), for values of γ = 10, 15, and 20. These correspond to (R_0, $[N_0]$) values of [(7 Å, 1.16 M); (10.5 Å, 0.34 M); (14 Å, 0.15 M)].

Self-Quenching in N2 and N10

One explanation for the observation that $I(t)$ decays as a sum of two exponential terms in N2 and N10 is that the naphthalene groups are distributed within the interphase domain in such a way that one can speak of regions of high $[N_s]$ and low $[N_l]$ local N concentration. These regions may correspond to N groups in pure PMMA $[N_s]$ or in interface region $[N_l]$ at the interphase domain, respectively. The situation is presented in Figure 1, where PIB microchannels may dilute the N concentration at the interface region; however, in pure PMMA region, N concentration may be higher.

Figure 6 represents a set of calibration curves that allow one to connect experimental τ_1/τ_0 and τ_s/τ_0 values with corresponding local concentrations $[N_l]$ and $[N_s]$. We have prepared a PIB–PMMA particle containing only 0.03% N groups. Its measured lifetime, 54 ns, can be set equal to τ_0. Values of τ_1/τ_0 and τ_s/τ_0 for powder samples of N2 and N10 are also indicated in Figure 6. If R_0, $[N_0]$, or γ were known for polymer-bound N-group fluorescence self-quenching, we could calculate the appropriate dependence of $\langle\tau\rangle/\tau_0$ on $[N]/[N_0]$, and directly obtain values of $[N_1]$ and $[N_s]$. We could, for example, guess that R_0 for this process is identical to that found for quenching of benzophenone triplets by naphthalene,[13] for which R_0 = 13 Å, $[N_0]$ = 0.18 M, and γ = 18. Alternatively, values of $[N_1]$ and $[N_s]$ can be calculated indirectly. We have noticed from the data in Figure 6 that the ratio of $[N_s]/[N_0]$ to $[N_1]/[N_0]$, for both N2 and N10, is independent of γ, at least for γ between 10 and 20. Thus, we calculate

$$[N_s]/[N_l] = 4.4 \quad \text{(N2)} \qquad (10a)$$

$$[N_s]/[N_l] = 2.6 \quad \text{(N10)} \qquad (10b)$$

Since A_l and A_s are proportional to the number of naphthalenes in the corresponding regions, we can calculate the ratio of the PMMA volumes V_1 and

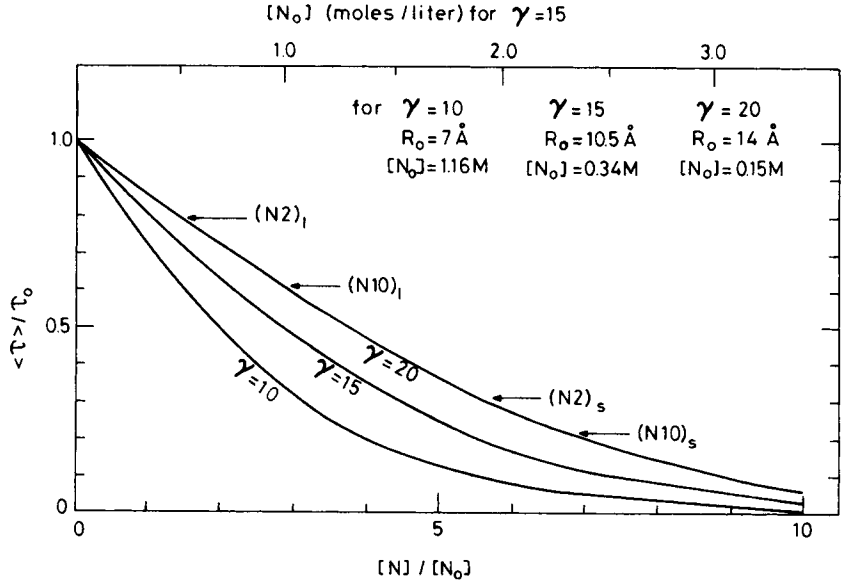

Figure 6 A plot of $\langle\tau\rangle/\tau_0$ vs. $[N]/[N_0]$ for a static quenching process as described by Inokuti and Hirayama. The curves are plotted from data in reference 13 for γ values indicated. The top axis is labeled with local concentration appropriate to the case of γ = 15.

Table I Lifetimes and Calculated Local [N] Concentrations in N2 and N10

	τ_s (ns)	τ_l (ns)	A_l/A_s
N2	17	43	2.69
N10	12	33	1.03

Calculated Local Concentrations (mol/liter)

	$[N_t]$	$[N_s]$	$[N_l]$	V_l/V_s
N2	0.31	1.08	0.24	11.8
N10	0.88	1.60	0.61	2.7

V_s, which contain low and high local naphthalene concentrations

$$\frac{V_l}{V_s} = \frac{A_l}{A_s}\frac{[N_s]}{[N_l]} \tag{11}$$

The total average concentration $[N_t]$ of N in the PMMA phase is given by the sum of the number of moles n_l, n_s of N groups in the l and s regions, divided by the sum of their respective volumes, V_l and V_s

$$[N_t] = \frac{n_l + n_s}{V_l + V_s} \tag{12}$$

Equation (12) can be written as

$$[N_l] = \frac{[V_l/V_s + 1][N_t]}{V_l/V_s + [N_s]/[N_l]} \tag{13}$$

which means that if $[N_t]$ is known, $[N_l]$ and $[N_s]$ can be calculated via Eqs. (13), (11), and (10).

Reasonable values of $[N_t]$ can be calculated from the experimentally determined composition of N2 and N10. One assumes that the N groups are located exclusively within the PMMA phase and that, that phase (at least in the dry powder samples) has the same density as bulk PMMA. These values and calculated $[N_s]$ and $[N_l]$ values are collected in Table I.

Volume Changes in Interphase Domain

Annealing of N2 and N10 leads to changes in the room temperature fluorescence decay rates (Figure 4) as well as in the A_l/A_s ratios (Figure 5). To interpret these data in terms of volume changes in the interphase domain, we must relate these short and long lifetime fluorescence decay components, after annealing at temperature T, $\tau_s(T)$, and $\tau_l(T)$, with the new N group concentrations $[N_s(T)]$ and $[N_l(T)]$. This would be straightforward if γ or R_0 for naphthalene self-quenching in PMMA were known. Because they remain unknown, these values have to be calculated indirectly by using the curves in Figure 6. We have found that the ratio of ratios

$$\frac{\tau(T)}{\tau_0} \Big/ \frac{\tau(25)}{\tau_0}$$

yield virtually identical values of

$$\frac{[N(T)]}{[N_0]} \Big/ \frac{[N(25)]}{[N_0]}$$

from each of the three curves in Figure 6. Furthermore, over a limited variation in $\tau(T)$, each of these curves can be approximated by a straight line. As shown in Figure 7, this assumption generates the following pair of relationships:

$$\frac{\tau_l(T)}{\tau_0} = 0.96 - 0.35\frac{N_l(T)}{N_l(25)} \tag{14a}$$

$$\frac{\tau_s(T)}{\tau_0} = 0.66 - 0.44\frac{N_s(T)}{N_s(25)} \tag{14b}$$

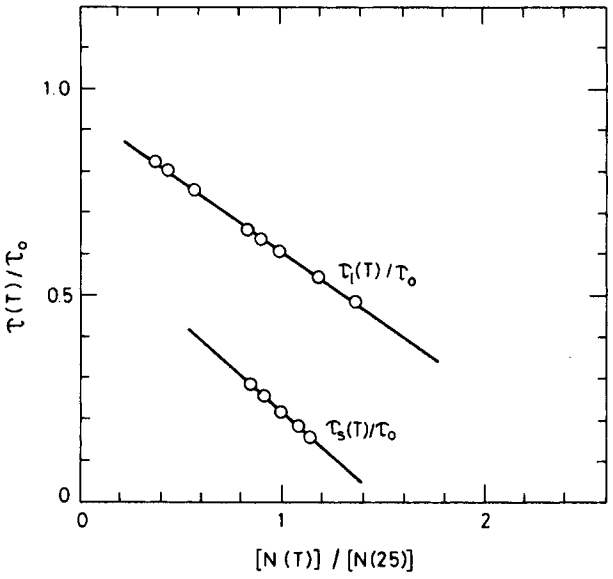

Figure 7 A plot of $\tau(T)/\tau_0$ vs. the ratio of $[N]/[N_0]$ to that $[N(25)]/[N_0]$ for a powder sample. The data are taken from Figure 6. For the upper line we plot $\tau 1(T)/\tau_0$ vs. $(N_l(T)/[N_0])/[N_l(25)]/[N_0] = [N_l(T)]/[N_l(25)]$. For the lower line we plot $\tau_s(T)/\tau_0$ vs. $(N_s(T)/[N_0])/[N_s(25)]/[N_0] = [N_s(T)]/[N_s(25)]$.

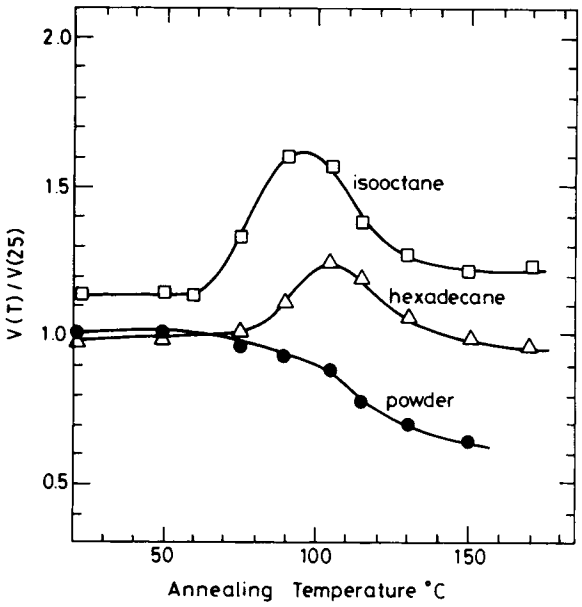

Figure 8 Plot of the annealing induced relative changes in volume of the interphase domain in N10 compared to that of initially prepared freeze-dried powder samples, $V(25)$ as calculated from Eq. (15): (□) isooctane dispersion; (△) hexadecane dispersion; (●) freeze-dried powder sample.

which permit $[N_l(T)]$ and $[N_s(T)]$ values to be calculated.

In order to examine the spectrum of swelling and contraction in the interphase domain of the material, we need to calculate changes in the total N group concentration $[N_t]$. Changes in $[N_t]$ are inversely proportional to the total volume of the interphase domain.

$$\frac{[N_t(25)]}{[N_t(T)]} = \frac{V(T)}{V(25)} \tag{15}$$

The $[N_t(T)]$ values can be calculated from Eq. (13), using experimental $(A_l/A_s)(T)$ values in conjunction with $[N_s(T)]$ and $[N_l(T)]$ obtained from Eq. (14). We plot $V(T)/V(25)$ vs. annealing temperature in Figure 8.

Annealing a powder sample of N10 causes a contraction of PMMA phase. Here, by contraction we mean that as PMMA phase relaxes at the interface region, volume of interface decreases locally by excluding PIB microchannels from that region (see Fig. 1) and $[N_l]$ increases. There is about an 8% decrease in volume for heating 3 h at 90°C, and nearly 36% decrease in volume for treatment at 150°C. Because the PMMA phase is glassy at room temperature, one anticipates that the magnitude of these phenomena would also depend upon the rate of cooling. We have not yet had a chance to verify this suggestion.

In isooctane and hexadecane, heating the dispersions above 60°C causes swelling in the interphase domain. The swelling is more pronounced in isooctane, amounting to about 42% increase in volume for samples heated at 90°C, which compares to 23% increase for hexadecane dispersions heated at 105°C. Annealing these samples at higher temperatures followed by cooling to 25°C results in deswelling of the interphase volume, which, in the case of hexadecane, results in a return to the initial value of V. Actually, here solvent molecules swell the PIB microchannels at the interface region and the local volume of the region increases. Subsequently, heat treatment above 105°C causes contraction of local interface volume due to exclusion of PIB microchannels from that region. One might infer from the intercepts of the $V(T)/V(25)$ plots that exposure of the solid dispersion to isooctane resulted in some interphase swelling prior to heating. Figure 9 shows the effect of swelling and contraction on $\tau_l(T)$ and

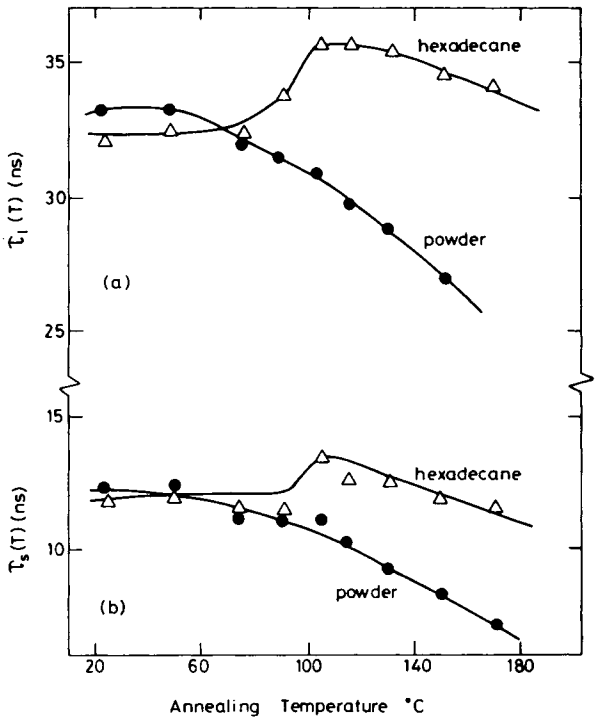

Figure 9 Plots of (a) $\tau_l(T)$ and (b) $\tau_s(T)$ for N10, measured at 25°C for samples annealed 3 h successively at each temperature indicated: (●) dry powder sample; (△) dispersion in hexadecane.

$\tau_s(T)$ lifetimes in the interface and pure PMMA regions, respectively. It is seen that, $\tau_l(T)$ times are effected more than $\tau_s(T)$ times, due to volume changes in the interphase domain.

In our previous work[1,2] the consequences of annealing of N2 and N10 on the rate and efficiency of fluorescence energy transfer were examined from N^* within the PMMA phase to anthracene (A) added as a solute in the continuous medium.

$$N^* + A \rightarrow N + A^* \qquad (16)$$

These works indicated nearly an order of magnitude increase in the room temperature rate of energy transfer after isooctane dispersions of the particles were annealed for 3 h at 140°C. The conclusions drawn from these results are that annealing increases the accessibility of N groups in the PMMA phase to solutes in isooctane, and the diffusion constant of A in the particle core increases to nearly equal that of A in isooctane itself.

Here, we are, thus, tempted to speculate that annealing at 100°C causes substantial solvent penetration into the interface region accompanied by some solvent-induced mixing of the PIB and PMMA phases within that region. Cooling the samples must cause solvent entrapment, leading to the extensive swelling observed for these samples. Heating to higher temperatures should promote similar phenomena. It is possible that upon cooling these samples that there would be adequate time for relaxation of the system leading to a PMMA phase composition where the mean N group separation was similar to that of the original sample.

History Effects on Swelling

Figure 10 shows the very curious result that the annealing-induced swelling of the PIB–PMMA particles is sensitive to the amount of time between sample preparation and the heat treatment. The dispersions in Figure 8 sat 1 month, sealed under vacuum in quartz tubes. When these experiments were repeated on a N10 sample stored for a year at room temperature, larger changes in $\tau_l(T)$ and $\tau_s(T)$ were observed, leading to the volume changes depicted in Figure 10. One also sees that a sample of N2 shows similar swelling behavior to that of N10 in isooctane. Here, we examined a sample that had been prepared for fluorescence measurements at room temperature for 5 months earlier and then carefully stored.

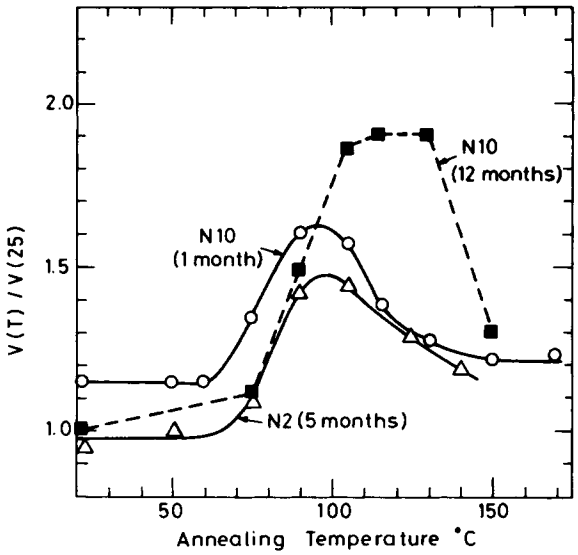

Figure 10 Plots of the relative changes in volume of the interphase domain in N10 (○, ■) and N2 (△) induced by sample annealing. The time between sample preparation and heat treatment is indicated on the graph.

We are not yet in a position to provide detailed explanations for these observations. History-dependent behavior is typical of polymers below T_g, and derives from the fact that the sample is prepared and frozen in a nonequilibrium state. In many of their applications, one does not control the time between NAD preparation and use. The techniques reported here would seem to give new insights into problems associated with the shelf life of these materials.

In conclusion, this work has shown that fitting fluorescence decay profiles to Eq. (2) is not a bad approximation in studying interphase domain of blendlike polymeric materials. The important point we wish to emphasize is that fluorescence decay analysis of appropriately labeled materials can provide quantitative insights into volume deformation of individual phases of these composite polymeric systems. One must take care to insure that only a single phase is, indeed, labeled. The experimental measurements are straightforward and make only minimal demands on the optical quality of the samples. We foresee the possibility that, in the near future, variations of the experiments described here will provide detailed descriptions of volume relaxation and history-dependent properties of many different blendlike composite materials.

I would like to thank Professor M. A. Winnik for providing me with his facilities and his stimulating ideas while I was at the University of Toronto.

REFERENCES

1. Ö. Pekcan, M. A. Winnik, L. E. Egan, and M. D. Croucher, *Macromolecules,* **16,** 699 (1983).
2. Ö. Pekcan, M. A. Winnik, and M. D. Croucher, *J. Polym. Sci., Polym. Lett.,* **21,** 1011 (1983).
3. Ö. Pekcan, M. A. Winnik, and M. D. Croucher, *Phys. Rev. Lett.,* **61,** 641 (1988).
4. Ö. Pekcan, L. S. Egan, M. A. Winnik, and M. D. Croucher, *Macromolecules,* **23,** 2210 (1990).
5. Ö. Pekcan, *Chem. Phys. Lett.,* **20,** 198 (1992).
6. M. A. Winnik, in *Polymer Surfaces and Interfaces,* J. Feast and H. Munro, Eds., Wiley, London, 1983.
7. Ö. Pekcan, *J. App. Polym. Sci.,* **49,** 151 (1993).
8. Ö. Pekcan, M. A. Winnik, and M. D. Croucher, *J. Colloid Interface Sci.,* **95,** 420 (1983).
9. Ö. Pekcan, (to appear).
10. M. A. Winnik, Ö. Pekcan, L. Chen, and M. D. Croucher, *Macromolecules,* **21,** 55 (1988).
11. F. Perrin, *Ann. Chem. Phys.,* **17,** 283 (1932).
12. A. Terenin and V. Ermolaev, *Izv. Akad. Nauk SSSR Ser. Fiz.,* **26,** 121 (1962).
13. M. Inokuti and F. Hirayama, *J. Chem. Phys.,* **43,** 1976 (1965).
14. D. L. Dexter, *J. Chem. Phys.,* **21,** 836 (1953).

Received April 25, 1994
Accepted October 6, 1994